

# A VIBRATION TECHNIQUE FOR NON-DESTRUCTIVELY ASSESSING THE INTEGRITY OF STRUCTURES

R. D. Adams†    P. Cawley†    C. J. Pye†    B. J. Stone†

A method of non-destructively evaluating the integrity of structures is described and applied to structures for which a one-dimensional analysis is satisfactory. It is shown how vibration measurements made at a single station in the structure can be used, in conjunction with a suitable theoretical model, to indicate both the location and the magnitude of a defect. Receptance analysis is used in this instance, but the principle is equally applicable to other techniques of mathematical analysis.

Experimental results are obtained on a variety of components, including straight prismatic bars, a doubly-tapered bar, and an automobile camshaft, excellent agreement between the predicted and actual damage sites being obtained. The axial mode of vibration is generally used, although some tests are also carried out successfully in torsion.

## 1 INTRODUCTION

In recent years, many new methods of non-destructive test have been developed. However, all of these tests have disadvantages as well as advantages, and there is no method which is universally applicable. One very common disadvantage is that the component under inspection must be investigated in a piece-wise manner. In some methods, such as ultrasonic C-scan, it is possible to automate this process, but this does not usually decrease the time required for inspection. Thus, any method which would enable a non-destructive test of a component to be made by simple measurements at one point on that component is a very attractive proposition. Depending on the degree of sophistication available or practicable, such a method may be used either to indicate that a component is damaged and leave it to more localized measurements to determine the nature of the damage, or to locate and to quantify the damage directly. Such a method requires a parameter to be found which will vary with damage in a specimen but which is not dependent on the point on the specimen at which the parameter is measured.

Adams *et al.* (1)‡ found that, with fibre-reinforced plastics, a state of damage could be detected by a reduction in stiffness and an increase in damping, whether this damage was localized, as in a crack, or distributed through the bulk of the specimen as many microcracks. Changes in stiffness, whether local or distributed, lead to changes in the natural frequencies of a vibrating system. Also, it is a property of a vibrating system that the resonant frequencies are functions of the physical and geometrical properties alone and are independent of the point of excitation (unless this is a node for any particular mode of vibration).

Thus, it was apparent that the natural frequency was a parameter which could satisfy the requirements already discussed. Since the stress distribution through a vibrating structure is non-uniform and is different for each natural frequency (mode), any localized damage would affect each mode differently, depending on the particular location of the damage. Thus, the measurement of the natural frequencies of a structure at two or more stages of its life

offers the possibility of locating damage in the structure and of determining the severity of the damage. If one set of frequencies was measured before the structure was put into service, subsequent frequency measurements could be used to test whether the structure was still sound.

This paper describes the theoretical and experimental work in which the concept was investigated. Since this was a first step, the scope of the work was restricted to simple systems consisting of straight bars but which could have cross-sections varying along the length of the bar.

### 1.1 Notation

$A$	Cross-sectional area
$E$	Young's modulus
$F$	Force amplitude
$f(x)$	$\partial(\beta_{xx} + \gamma_{xx})/\partial\omega$
$K$	Spring stiffness
$l$	Total length of bar
$x$	Length of a section of bar
$\alpha$	Temperature coefficient of linear expansion
$\alpha_E$	Temperature coefficient of modulus
$\beta$	Receptance of system B
$\gamma$	Receptance of system C
$\theta$	Temperature
$\lambda$	$\omega\sqrt{\rho/E}$
$\rho$	Density
$\omega$	Frequency

### Subscripts

$n, p, q$	Mode numbers
$s, x$	Positions on bar

## 2 THEORY

### 2.1 Background

Since the object of the work was to develop a simple non-destructive test, the choice of the modes of vibration was restricted mainly to axial vibration and the theory has been developed for axial modes. However, some torsional modes were considered, and it should be remembered that the theoretical expressions for axial vibration have torsional equivalents. Flexural modes were considered unnecessarily complicated at this stage, though the

The MS. of this paper was received at the Institution on 1 July 1977 and accepted for publication on 1 December 1977.

† University of Bristol.

‡ References are given in the Appendix.

concept could be, and is being, modified to incorporate them.

The theoretical analysis of the axial vibration of a bar with localized damage requires a model of the damage. There are many different types of damage and a detailed analysis of each and every type would be of little value, whereas it was considered that a macroscopic model might cover most possibilities. Two different models were considered. In the first, the damaged section was taken as a short section with reduced modulus, thus requiring two parameters for its definition (length and modulus). In the second, the damage was represented by the insertion of a massless spring of infinitesimal length, which requires only the spring stiffness to define the damage. As it may be shown that the two models are equivalent when the length of the section with reduced modulus is small, the spring model was chosen as it is the simpler of the two.

The theory was developed neglecting damping, since only changes in natural (or resonant) frequency were being considered. The theoretical analysis involves the use of receptances, and it is thus necessary to define the axial receptance of a bar. If a sinusoidal force,  $F_s e^{i\omega t}$ , is applied to the end of a bar specified by the subscript  $s$ , and the resulting sinusoidal displacement at  $s$  is  $X_s e^{i\omega t}$ , then the direct receptance at  $s$  of the bar is defined as  $\beta_{ss} = X_s/F_s$ ; thus  $\beta_{ss}$  will vary with frequency and attains maximum values at the resonant frequencies of the bar.

For the structures considered in this work, exact expressions for the appropriate receptances could be obtained. With more complex structures, it might be necessary to determine the receptances by approximate methods, for example, finite elements. The work is now being extended to structures for which this approach is necessary.

**2.2 Method of damage location**

Consider a damaged bar as modelled in Fig. 1. Suppose the damage to be located at some unknown axial position  $x$ , the value of which is the object of the analysis (i.e. the position of the damage). Further, let the spring representing the damage have a stiffness  $K_x$ . This is also unknown and is a measure of the severity of the damage. If  $K_x$  is infinite, there is no damage, while decreasing values of  $K_x$  indicate increasing damage.

If the parts of the bar on either side of the damage are defined as B and C, having receptances  $\beta$  and  $\gamma$  respectively, then the natural frequencies of the damaged bar are such that the following equation is satisfied (2):

$$\beta_{xx} + \gamma_{xx} + \frac{1}{K_x} = 0 \tag{1}$$

where  $\beta_{xx}$  is the direct receptance of bar B at the position  $x$ , and  $\gamma_{xx}$  is the direct receptance of bar C at  $x$ . These receptances have values determined by the frequencies which satisfy (1) and the physical and geometrical properties of the bars.

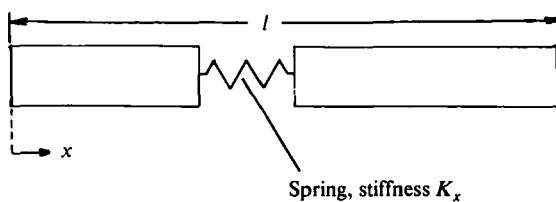


Fig. 1. Structure with spring representation of damage

Now for an undamaged bar,  $K_x = \infty$  and equation (1) reduces to

$$\beta_{xx} + \gamma_{xx} = 0. \tag{2}$$

For the  $n$ th mode of such an undamaged bar having a natural frequency  $\omega_n$ ,

$$(\beta_{xx} + \gamma_{xx})_{\omega=\omega_n} = 0 \tag{3}$$

If such a bar were damaged at  $x$ , so that the natural frequency of the  $n$ th mode is reduced to  $\omega_n - \Delta\omega_n$ , then the spring stiffness which models the system is given by

$$\frac{1}{K_x} = -(\beta_{xx} + \gamma_{xx})_{\omega=\omega_n-\Delta\omega_n} \tag{4}$$

Now, if only one mode were considered and the values of  $\omega_n$  and  $\Delta\omega_n$  were known, it would be possible, if the variations of  $\beta_{xx}$  and  $\gamma_{xx}$  were known as functions of  $\omega$  and  $x$ , to determine the value of  $K_x$  at any value of  $x$  which would cause the natural frequency,  $\omega_n$ , to decrease to  $\omega_n - \Delta\omega_n$ . However, it is required to determine the actual values of  $x$  and  $K_x$ , and this may be achieved if the change in frequency of two modes is considered. If  $K_x$  does not vary with frequency, then the value of  $x$  required is that which will yield the same value of  $K_x$  from the measured change in frequency of each mode.

Thus, if the modes corresponding to  $n = p$  and  $n = q$  are used and  $(\omega_p - \Delta\omega_p)$  and  $(\omega_q - \Delta\omega_q)$  are measured, i.e. the damaged natural frequencies, then

$$\frac{1}{K_x} = -(\beta_{xx} + \gamma_{xx})_{\omega=\omega_p-\Delta\omega_p} = -(\beta_{xx} + \gamma_{xx})_{\omega=\omega_q-\Delta\omega_q} \tag{5}$$

A graph superposing  $-(\beta_{xx} + \gamma_{xx})_{\omega=\omega_p-\Delta\omega_p}$  and  $-(\beta_{xx} + \gamma_{xx})_{\omega=\omega_q-\Delta\omega_q}$  plotted against  $x$  will therefore give the possible damage site(s) and associated value of  $K_x$  at the intersection(s) of the curves.

**2.3 Example of a straight bar**

In the case of a bar of constant cross-section, the appropriate receptances for damage at location  $x$  are (2)

$$\beta_{xx} = \frac{-\cos \lambda x}{AE\lambda \sin \lambda x}; \quad \gamma_{xx} = -\frac{\cos \{\lambda(l-x)\}}{AE\lambda \sin \{\lambda(l-x)\}} \tag{6}$$

where the symbols have the meanings given in Section 1.1.

Substituting these values in equation (4) yields

$$\frac{1}{K} = \frac{\cos \lambda x}{AE\lambda \sin \lambda x} + \frac{\cos \{\lambda(l-x)\}}{AE\lambda \sin \{\lambda(l-x)\}}$$

or

$$\frac{EA}{K} = \frac{1}{\lambda} \left( \cot \lambda x + \cot \{\lambda(l-x)\} \right) \tag{7}$$

For the first three modes of such a bar, Fig. 2 shows the right-hand side of equation (7) plotted against position  $x$ , for values obtained in a particular experimental situation. The frequency,  $\omega$ , used in the evaluation of the receptances is the frequency of the appropriate mode after damage. The possible damage sites are given by the intersections of the curves for the different modes. It will be observed that two damage sites are indicated. The use of the third mode does not eliminate one of the sites, as the

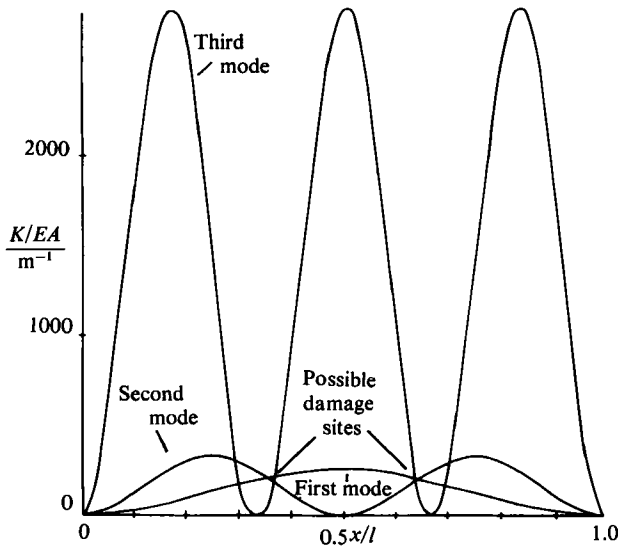


Fig. 2. Damage location in a straight bar

symmetry of the bar prohibits this. With asymmetrical structures, the use of any two modes will give two or more possible damage sites, while the use of additional modes will reduce this.

**2.4 Determination of material parameters**

The evaluation of the right-hand side of equation (4) requires the knowledge of the dimensions and the velocity of sound of the bar. Quoted values of the material properties are not sufficiently accurate for this purpose. The problem can be overcome by using the undamaged natural frequencies of the bar to determine an effective value of Young's modulus, *E*. The dimensions of the bar are measured and a published value of density is assumed. The natural frequency equation for the undamaged bar is then solved, using an iterative method to give an effective value of Young's modulus for the bar such that the theoretical undamaged frequency is equal to the measured value. Effective values of Young's modulus are thus found for each mode.

This approach is very useful in that errors in the receptance model of the bar are, to a large extent, eliminated by compensation in the value of Young's modulus. In fact, the value of *E* determined computationally is a useful check on the accuracy of the model.

**2.5 Further development of the theory**

If  $\beta_{xx}$  and  $\gamma_{xx}$  are continuous functions of  $\omega_n$  (this is normally the case) then, for small values of  $\Delta\omega_n$ ,

$$(\beta_{xx} + \gamma_{xx})_{\omega = \omega_n - \Delta\omega_n} =$$

$$(\beta_{xx} + \gamma_{xx})_{\omega = \omega_n} - \left[ \frac{\partial}{\partial \omega} (\beta_{xx} + \gamma_{xx})_{\omega = \omega_n} \right] \Delta\omega_n$$

Substituting from (3) and (4) yields

$$\frac{1}{K_x} = \left[ \frac{\partial}{\partial \omega} (\beta_{xx} + \gamma_{xx})_{\omega = \omega_n} \right] \Delta\omega_n \tag{8}$$

that is,

$$\frac{1}{K_x} = f(x)_n \Delta\omega_n \tag{9}$$

where  $f(x)_n = \partial/\partial\omega(\beta_{xx} + \gamma_{xx})_{\omega = \omega_n}$  and is a function of the particular bar, *x* and  $\omega_n$ , but which may be determined mathematically.

If, again, it is assumed that  $K_x$  is independent of frequency and modes *p* and *q* are considered, then

$$\frac{1}{K_x} = f(x)_p \Delta\omega_p = f(x)_q \Delta\omega_q$$

Thus, the position of the damage site, *x*, is such that *x* satisfies the equation

$$f(x)_p \Delta\omega_p = f(x)_q \Delta\omega_q$$

Now,  $f(x)_p/f(x)_q$  may be calculated and plotted against *x*. If the ratio of the frequency changes,  $\Delta\omega_q/\Delta\omega_p$ , is measured, the damage site is given by the value of *x* at which  $\Delta\omega_q/\Delta\omega_p$  is equal to  $f(x)_p/f(x)_q$ .

As an example, consider again the straight bar.

Differentiating the expressions for  $\beta_{xx}$  and  $\gamma_{xx}$  in equation (6) gives

$$\frac{\partial}{\partial \omega} (\beta_{xx} + \gamma_{xx})_{\omega = \omega_n} =$$

$$\frac{\frac{x}{l} \operatorname{cosec}^2\left(\frac{n\pi x}{l}\right) + \left(1 - \frac{x}{l}\right) \operatorname{cosec}^2\left(n\pi\left(1 - \frac{x}{l}\right)\right)}{\frac{AE n \pi}{l^2} \sqrt{\frac{E}{\rho}}}$$

Thus,

$$\frac{f(x)_p}{f(x)_q} =$$

$$\frac{\left[ \frac{x}{l} \operatorname{cosec}^2\left(\frac{p\pi x}{l}\right) + \left(1 - \frac{x}{l}\right) \operatorname{cosec}^2\left(p\pi\left(1 - \frac{x}{l}\right)\right) \right] q}{\left[ \frac{x}{l} \operatorname{cosec}^2\left(\frac{q\pi x}{l}\right) + \left(1 - \frac{x}{l}\right) \operatorname{cosec}^2\left(q\pi\left(1 - \frac{x}{l}\right)\right) \right] p}$$

If  $f(x)_p/f(x)_q$  is plotted against *x/l*, a universally applicable chart is obtained for uniform straight bars which is independent of their material properties and dimensions. For such a bar, if the frequency change in the modes *p* and *q* is measured, the damage may be located. Fig. 3 shows such a chart which incorporates the various combinations of the first, second and third modes. Thus, for example, if the frequency changes in the first and second modes were such that  $\Delta\omega_2/\Delta\omega_1 = 1.0$ , then the damage site would be at  $x/l = 0.385$  or  $x/l = 0.615$ , two positions being possible because of symmetry.

The analysis has been illustrated with a constant-diameter bar, but is applicable to bars having more complex variations in cross-section. Stepped bars have been examined, as have tapered bars. The receptances of tapered bars are given in (3). In fact, the method is applicable to any bar for which  $\beta_{xx}$  and  $\gamma_{xx}$  may be

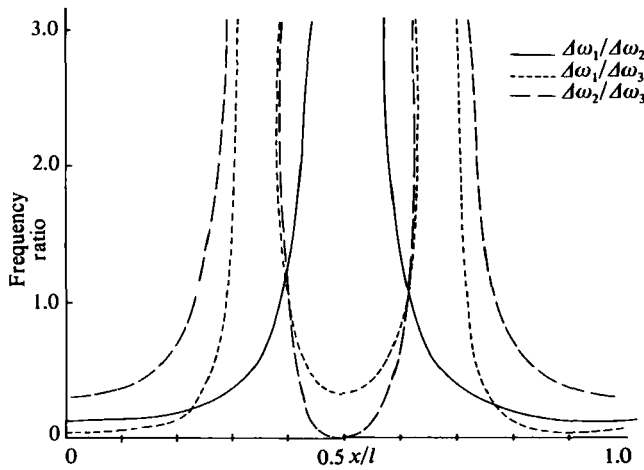


Fig. 3. Chart for location of damage in a straight bar

obtained as functions of  $x$ . For the more complicated bars, the mathematical derivation of  $\partial(\beta_{xx} + \gamma_{xx})_{\omega=\omega_n}/\partial\omega$  is not practicable and the following method has been adopted.

From equation (9), it follows that

$$f(x)_n = \frac{1}{K_x \Delta\omega_n}$$

It is convenient to use a computer to determine, for the  $n$ th mode and a specific value of  $\Delta\omega_n$ , the value of  $K_x$  at the position  $x$  which would give the reduction in frequency,  $\Delta\omega_n$ . Then,  $f(x)_n$  is easily computed and the graph of  $f(x)_n/f(x)_0$  against  $x$  may be determined.

The production of a chart has the advantage that it is applicable to any geometrically similar structure and that the possible damage locations may be read directly off it without the need for further computation. In cases where the explicit differentiation of the expressions for  $\beta_{xx}$  and  $\gamma_{xx}$  is not practicable, the computational effort required to produce the chart is considerably greater than that required to produce curves of the type shown in Fig. 2, if only one structure of this type is to be tested. In situations where several similar structures were to be tested, use of the chart would give a significant saving in computer time. The chart also has the advantage that it gives a direct indication of the damage site without the need for further computation. It is thus considerably more convenient unless on-line computing facilities are available. Most of the results quoted in this paper were produced using the method of Section 2.2. This method was chosen in preference to the chart because usually only one structure of a given type was to be tested and on-line computing facilities were available. There are many situations in industry, however, where use of the chart would be more appropriate.

### 2.6 Temperature effects

The method of damage detection and location requires the measurement of the difference between the undamaged and damaged natural frequencies of the structure. Since the second set of frequencies will often be measured after a period of time in service, it is probable that the ambient temperature will have changed. It is therefore necessary to correct the natural frequencies to take account of any tem-

perature change. This may be done using the method described by Adams and Crippendale (4).

The axial resonant frequency of a straight bar of length  $l$  is given by

$$\omega_n = \frac{\pi}{l} \sqrt{\frac{E}{\rho}} \quad (10)$$

From (10), it can be shown that

$$\frac{\delta\omega_n}{\omega_n} = -\frac{\delta l}{l} + \frac{1}{2} \frac{\delta E}{E} - \frac{1}{2} \frac{\delta\rho}{\rho} \quad (11)$$

where  $\delta j$  is an increment in parameter  $j$ .

If the temperature of the bar changes by an amount  $\delta\theta$ , then

$$\frac{\delta l}{l} = \alpha\delta\theta \quad (12)$$

and

$$\frac{\delta\rho}{\rho} = -3\alpha\delta\theta \quad (13)$$

where  $\alpha$  is the coefficient of linear expansion of the material.

It may be assumed that, for small changes in temperature, the variation of Young's modulus with temperature is linear. Thus,

$$\frac{\delta E}{E} = \alpha_E \delta\theta \quad (14)$$

where  $\alpha_E$  is the temperature coefficient of modulus of the material. For most materials,  $\alpha_E$  is negative.

Combining equations (11), (12), (13) and (14) gives

$$\delta\omega_n = \frac{\omega_n}{2} (\alpha + \alpha_E) \delta\theta \quad (15)$$

The temperature correction,  $\delta\omega_n$ , may thus be obtained from the temperature change between the two sets of measurements using published values of  $\alpha$  and  $\alpha_E$ . Tests have shown that these values are sufficiently accurate for this purpose.

Equation (15) was also used in the case of bars of non-uniform cross-section and was found to be an adequate approximation. The damaged frequencies quoted in Tables 1-4 were all corrected for temperature changes.

### 3 EXPERIMENTAL INVESTIGATION

The basic requirement of the method is reproducibly to determine several (usually the first two or three) natural frequencies of the structure under consideration. It does not matter whether the frequencies measured are the exact frequencies (assuming idealized boundary conditions) provided that they are reproducible and the mode shape is not greatly altered from that predicted by the theoretical model. Therefore, a variety of methods of exciting and detecting the vibrational response may be used as this criterion is easily met.

Table 1. Results from aluminium bar

Total length of beam (m)	First mode		Second mode		Third mode				Average calculated distance of damage from end (m)	EA/K (10 <sup>-3</sup> m)
	Undamaged frequency (Hz)	Frequency reduction $\Delta F_1$ (Hz)	Undamaged frequency (Hz)	Frequency reduction $\Delta F_2$ (Hz)	$\frac{\Delta F_2}{\Delta F_1}$	Undamaged frequency (Hz)	Frequency reduction $\Delta F_3$ (Hz)	$\frac{\Delta F_3}{\Delta F_1}$		
0.519 96	4770	39	9 536	0	0	14 294	118	3.03	0.261	4.3
0.493 14	5029	45	10 055	5	0.111	15 071	129	2.87	0.262	4.5
0.464 50	5340	50	10 675	17	0.340	16 001	115	2.30	0.260	4.5
0.432 12	5740	52	11 474	43	0.827	17 200	65	1.25	0.260	4.4
0.403 06	6144	53	12 283	83	1.57	18 412	15	0.283	0.260	4.4
0.369 24	6717	55	13 428	158	2.87	20 192	58	1.05	0.264	4.8
0.336 52	7370	52	14 734	198	3.80	22 086	230	4.42	0.263	4.7
0.302 08	8210	17	16 414	151	8.88	—	—	—	0.283	13.0
0.269 82	9192	0	18 376	32	$\infty$	—	—	—	Damage at end of bar	—

Actual distance of damage from end = 0.260 m.

Table 2. Results from G.F.R.P. tube

Type of damage	Natural frequencies (Hz)			Average calculated distance of damage from end (m)	EA/K (10 <sup>-3</sup> m)
	First mode	Second mode	Third mode		
Undamaged	2916	5916	9010	—	—
Crushed in vice	2912	5915	8995	0.205	0.96
Further crushing	2909	5915	8983	0.202	1.48
Further crushing at a different circumferential position	2906	5915	8983	0.206	2.4
Damage in three-point bending	2894	5915	8936	0.212	4.5
Further damage in three-point bending	2886	5913.5	8857	0.207	6.4

Actual distance of damage from end = 0.202 m.

Table 3. Results from tapered bar

Percentage of area removed	Natural frequencies (Hz)			Average calculated distance of damage from large end (m)	EA/K (m)
	First mode	Second mode	Third mode		
0	4668.9	8192.7	11 665.0	—	—
1.4	4668.8	8191.9	11 664.0	0.137	0.0254
2.8	4668.7	8190.4	11 662.1	0.132	0.0746
4.2	4667.8	8185.7	11 657.0	0.136	0.2198

Actual distance of damage from large end = 0.136 m.

The resonant frequency was assumed to be that at which maximum amplitude occurred. This is a reasonable criterion to use with low damping structures and is much easier to apply than the 90° phase-shift criterion. A six-figure frequency read-out was desirable though, in many cases, five figures were sufficient. A block diagram of a typical experimental arrangement is shown in Fig. 4.

A series of tests was designed to investigate the accuracy of the method on simple, essentially one-dimensional, structures vibrating longitudinally.

### 3.1 Aluminium bar with a saw cut

In the first test, the 'structure' consisted of an aluminium bar of rectangular section. After the initial frequencies of the bar had been measured, it was damaged by two saw cuts on opposite sides of the bar at the mid-section, each cut removing about 15 per cent of the cross-sectional area. The frequencies of the damaged bar were then measured.

The position of the damage relative to the centre of the bar was then changed by cutting a short length from one end. The undamaged natural frequencies of the new system were calculated from simple length proportions since, provided the ends remained square after shortening, the length could be measured with similar accuracy to the natural frequencies. This process was continued until the damage zone was almost at the end of the bar. The results from these tests are shown in Table 1. It can be seen that the ratios of the frequency changes in the three modes change as the damage moves towards the end of the bar. The damage site was located accurately except when it was near the end of the bar, when the change in first-mode frequency was negligible. Unfortunately, it was not possible to use the third mode in the last two tests because the frequency was above the limit of the equipment used. Since the stress at the end of the bar was zero in all modes,

Table 4. Camshaft results

	Frequencies (Hz)			Frequency reduction (Hz)			Average calculated distance from end (m)	Percentage of area removed	EA/K (m)
	Mode 1	Mode 2	Mode 3	Mode 1	Mode 2	Mode 3			
Undamaged	5577.7	11 207.0	17 977.7	—	—	—	—	—	—
First cut	5572.7	11 206.9	17 966.6	5.0	0.1	11.1	0.164	3.5	0.61
Second cut	5557.6	11 206.5	17 927.6	20.1	0.4	50.1	0.161	8.0	3.2

Actual distance of damage from end = 0.162 m.

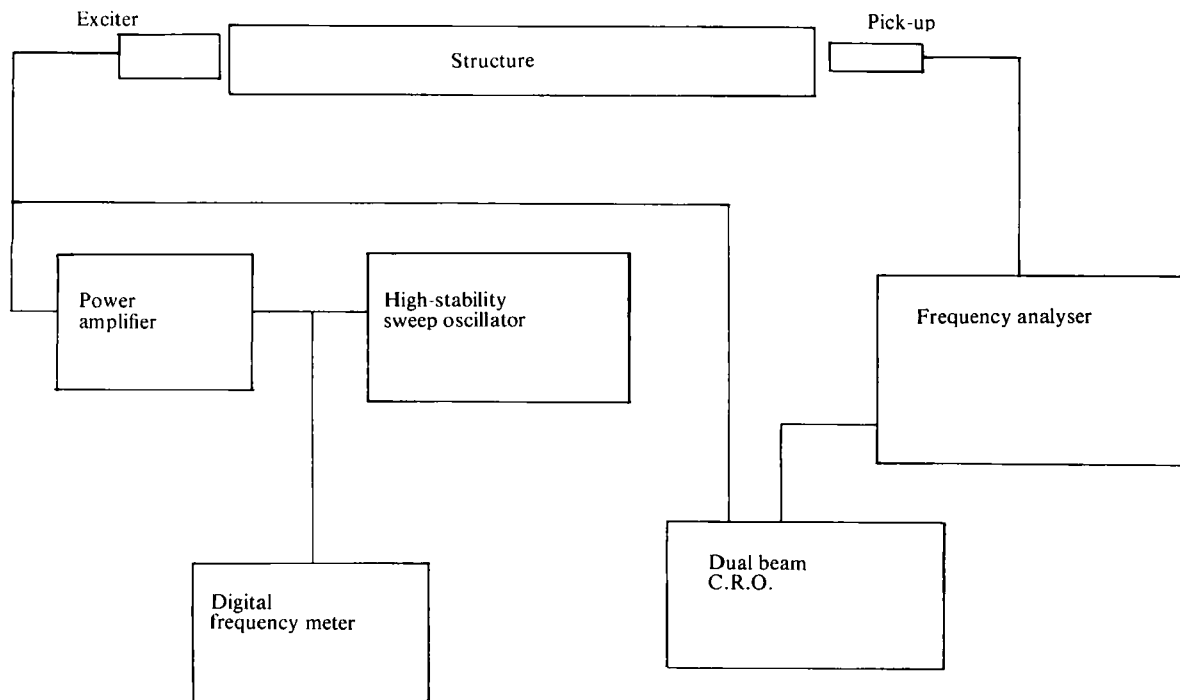


Fig. 4. Block diagram of apparatus

any damage there will have little effect on the natural frequencies, so the damage location will be less accurate when it is sited near the end. An improvement in accuracy could be expected if higher modes were used. The value of  $EA/K$  obtained varied very little as the beam was shortened, indicating constant severity of damage, which is as it should be.

Since a beam without an end mass is a symmetrical system, the method always yields two possible damage sites symmetrically disposed with respect to the mid-section of the beam. For simplicity, only the site near the actual damage position is given in Table 1. Typical curves showing the two possible damage sites are shown in Fig. 2. The curves shown in Fig. 2 are for the test in which the length of the bar was 0.4031 m.

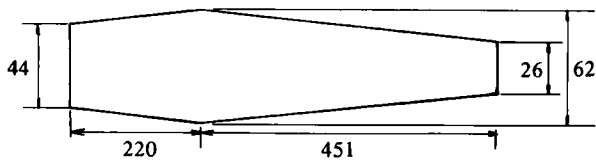
### 3.2 Tests on bars with more realistic forms of damage

Having verified the theory on a simple system, some tests were carried out on systems with types of damage more likely to be encountered in real components. An aluminium beam (380 mm × 10 mm × 5 mm) was vibrated in flexure to produce a fatigue crack at the mid-section. It was found that the crack could be located as easily as had been the saw-cut damage. This even applied to a crack which was not visible to the naked eye but

could be seen under a microscope after the vibration tests had indicated both that it existed and where it was located.

Several tests were carried out on filament wound glass-fibre-reinforced plastic (G.F.R.P.) tubes which were damaged by crushing in a vice and by loading in three-point bending, both of which produced a diffuse area of damage rather than a single crack. The results from one of these tubes (which had an aluminium endpiece glued on to carry the excitation system) are shown in Table 2. The analysis for the composite tubes was identical to that for an isotropic material since purely longitudinal motion was considered. This meant that the longitudinal modulus was the only relevant elastic constant. The aluminium endpiece was modelled as a point mass at the end of the tube. It can be seen that the damage was always located fairly accurately and that the value of  $EA/K$  increased as the amount of damage was increased, indicating that this parameter may be used as an indication of the severity of damage.

This structure was no longer symmetrical about the mid-section (due to the endpiece), but the degree of asymmetry was insufficient for the damage site to be determined uniquely—two possible sites were again indicated. For simplicity, only the site near the actual damage position is shown in Table 2.



All dimensions in mm

Fig. 5. Dimensions of tapered bar

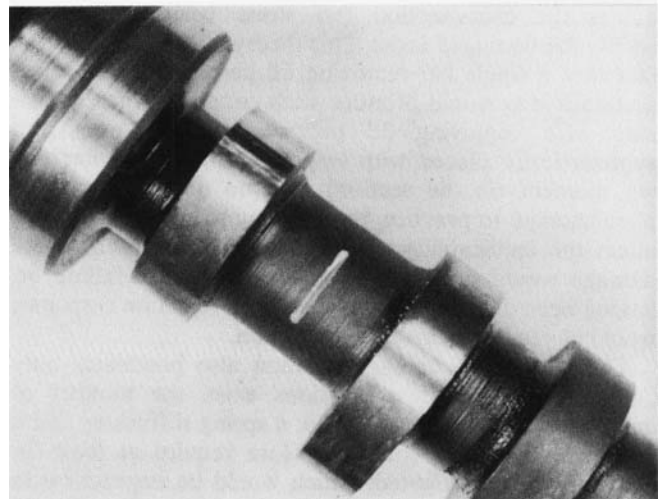
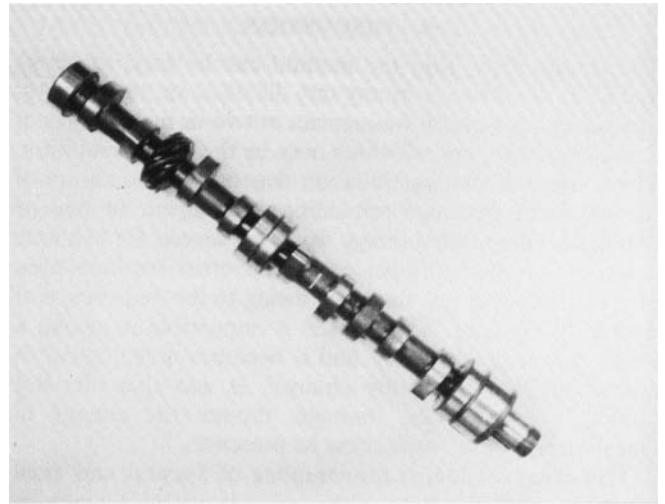


Fig. 7. Photographs of damaged camshaft

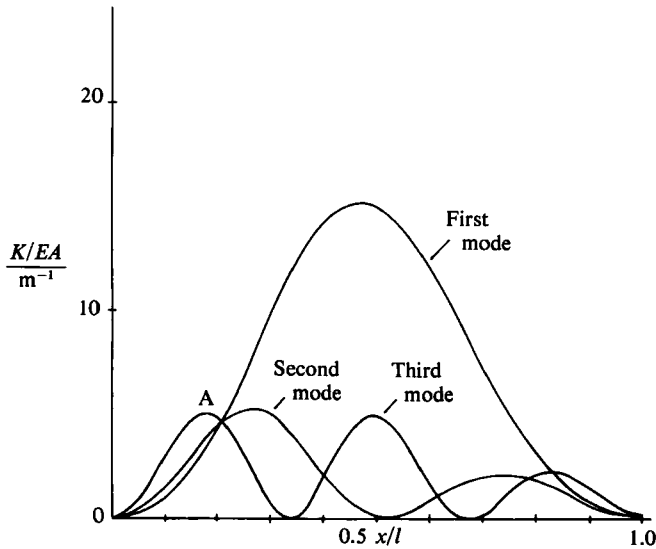


Fig. 6. Damage location in tapered bar

**3.3 Tests on a tapered bar**

In order to test the applicability of the method to systems which were not of uniform cross-section, the tapered steel bar shown in Fig. 5 was tested. In view of the difficulty of producing a fatigue crack in a bar of this size, it was damaged with a series of saw-cuts. The results are given in Table 3 and a typical set of curves is shown in Fig. 6.

With the smallest cuts, the change in first-mode frequency was too small to be measured accurately, so the damage location was achieved using second and third modes. In this case, the structure was sufficiently asymmetrical for the damage site to be uniquely specified. The curves presented in Fig. 6 clearly show that the damage is at site A. Again, the value of  $EA/K$  increased as the severity of the damage was increased.

**3.4 Tests on a camshaft**

The final series of tests was carried out on an automobile camshaft. Although this was not essentially a one-dimensional structure, it could be modelled as such by assuming it to be a straight bar made up of a series of cylinders of different diameters, the centres of these cylinders all lying on the same axis.

The camshaft was initially damaged by a single, shallow saw-cut of depth 1.7 mm. This corresponded to a 3.5 per cent reduction in area of that section of the bar. The results for this amount of damage are given in the second line of Table 4. The size of the cut was then increased, resulting in an 8 per cent reduction in area of that section of the bar. A photograph of the actual camshaft used is shown in Fig. 7, which also gives a close-up view of the extended saw-cut. The results for this test are given in the

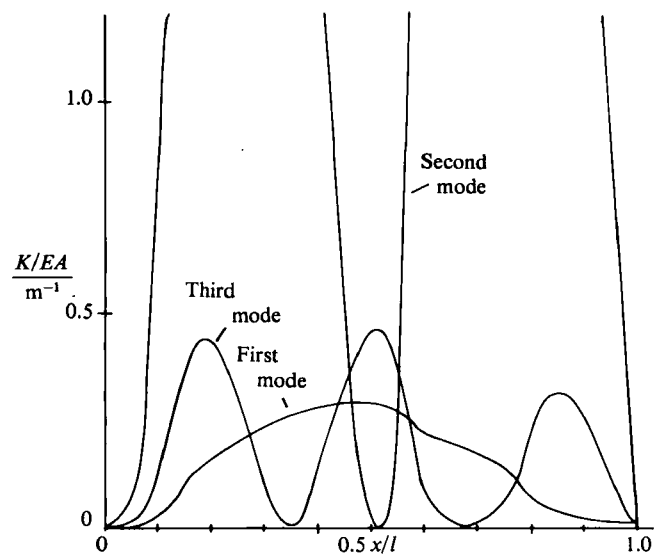


Fig. 8. Damage location in camshaft

third line of Table 4 and the corresponding damage location curves are given in Fig. 8. It can be seen that the method has again been used successfully to locate the damage site and give an indication of the severity of the damage.

#### 4 DISCUSSION

The results show that the method can be used to detect and to locate damage in any one-dimensional structure by measuring the natural frequencies at two or more stages of damage growth, one of which may be the virgin condition. The method of damage location depends on the nature of the vibration response remaining unchanged. In one or two cases where the damage was very severe, for example a saw-cut removing 60 per cent of the cross-sectional area of a bar, this was not the case, owing to the occurrence of double resonances. This makes it impossible to define a single resonant frequency and it becomes meaningless to talk about 'the frequency change'. It was therefore not possible to locate the damage, though the change in vibration response could show its presence.

This effect is due to the coupling of flexural and axial vibration, since the stress distribution is no longer uniform across the cross-section (no stress being transmitted across the damaged area). This theory is supported by the fact that a single cut removing 60 per cent of the cross-sectional area would produce such coupling, whereas two cuts each removing 30 per cent of the area and symmetrically placed with respect to the centre line (no net moment on the section) give no double resonance phenomenon. In practice, the coupling would probably not affect the applicability of the method, since such severe damage would probably have already caused failure or, having been detected by the change in vibration response, would be readily located on inspection.

The method of damage location also postulates only one damage site. If  $n$  locations exist, the number of unknowns would increase to  $2n$ ,  $n$  spring stiffnesses and  $n$  positions. Solution would therefore require at least  $2n$  modes to be investigated, which would be impractical in many cases. The presence of damage would, however, still be detected by a decrease in the resonant frequencies, so the failure to locate the damage accurately in the unlikely event of there being more than one major site is not too important.

The tests indicated that the minimum amount of damage which could be detected is that which is equivalent to the removal of about 1 per cent of the cross-sectional area. The limiting factor was the accuracy to which the resonant frequencies could be reproduced; about  $\pm 0.1$  Hz in 10 000 Hz has been achieved in these tests.

The method has the advantage that it is no less accurate, nor does it involve more labour, when testing large structures; a crack removing the same percentage of the cross-sectional area is as easy to detect in a large bar as in a very small one. This compares favourably with techniques such as ultrasonics and radiography where the whole surface must be scanned.

The technique can also be used on structures that are inaccessible over most of their surface; only one access point is required, since both excitation and pick-up may be at the same point.

The tests on the camshaft indicated that great accuracy in the receptance model was not necessary. In this case, it was adequate to treat the cam lobes as having the effect of a uniform increase in the diameter of the shaft. The critical factor was that the mode shapes had to be adequately approximated, resulting in the frequencies of the modes being in the correct ratios. The difference in the values of  $E$  obtained for the three modes gives some idea

of the accuracy of the model. With a straight bar, where the model should be very accurate, the  $E$ -values agreed to within about 0.25 per cent, whereas with the camshaft the agreement was only to about 4 per cent.

Most of the work done so far involved axial vibration with damage in a plane normal to the longitudinal axis. A longitudinal shear crack would have little effect on the axial stiffness and so would not affect the axial natural frequencies. If this type of damage were suspected, it would be necessary to use torsional or flexural vibration to detect it. The expressions produced for axial vibration have torsional analogues and a few tests were done on an aluminium tube using torsional vibration. The results were very satisfactory, and there is no reason why torsion should not be used in the same way as axial vibration. It is a matter of practical experience that torsional oscillations are more difficult to excite and to detect in bars than are axial oscillations. The use of flexural motion requires a different set of equations, but there is no reason why the principle should not be extended to this case and, indeed, work is now being carried out on this topic.

The tests on the G.F.R.P. tubes indicated that this technique has considerable potential for use with composite materials. Some difficulty has been experienced in applying ultrasonic techniques to these materials because of their non-homogeneous nature, high attenuation, and also because they often fail in shear, producing a 'zero volume' crack that has no effect on the propagation of ultrasonic waves.

The results presented in Tables 2, 3 and 4 show that the value of the 'damage parameter',  $EA/K$ , increases with increasing severity of damage. In situations where the probable orientation of damage is known, the value of this parameter could be used as a measure of the severity of damage. The method may therefore be used to detect, locate and quantify damage.

#### 5 CONCLUSIONS

A non-destructive test has been developed which is applicable to all structures for which a one-dimensional analysis is an adequate approximation. The method can be used to detect and locate damage without the need for access to the whole structure, and it has the further advantage that the labour involved is not increased with increasing size of the structure. The testing technique is simple, quantifiable and offers the possibility of automation.

#### APPENDIX

##### REFERENCES

- (1) ADAMS, R. D., WALTON, D., FLITCROFT, J. E. and SHORT, D. 'Vibration testing as a nondestructive test tool for composite materials', *Composite Reliability* ASTM STP 580, American Society for Testing and Materials, 1975, 159-175.
- (2) BISHOP, R. E. D. and JOHNSON, D. C. *The mechanics of vibration* 1960 (Cambridge University Press).
- (3) STONE, B. J. 'The receptances of tapered bars' (to be published).
- (4) ADAMS, R. D. and COPPENDALE, J. 'Measurement of the elastic moduli of structural adhesives by a resonant bar technique', *J. mech. Engrng Sci.* 1976 **18** (No. 3).